Virology 538 (2019) 61–70

Contents lists available at ScienceDirect

Virology

journal homepage: www.elsevier.com/locate/virology

Attenuation of a virulent swine acute diarrhea syndrome coronavirus strain via cell culture passage

Y. Sun[1], J. Cheng[1], Y. Luo, X.L. Yan, Z.X. Wu, L.L. He, Y.R. Tan, Z.H. Zhou, Q.N. Li, L. Zhou, R.T. Wu, T. Lan[*], J.Y. Ma[**]

College of Animal Science, South China Agricultural University, Guangzhou, China

ARTICLE INFO

Keywords:
SADS-CoV
Attenuation
Cell adaptation
Genomic analysis
Pathogenicity
NS7a/7b

ABSTRACT

Swine acute diarrhea syndrome coronavirus (SADS-CoV) is a newly identified enteric alphacoronavirus that causes fatal diarrhea in newborn piglets in China. Here, we propagated a virulent strain SADS-CoV/CN/GDWT/2017 in Vero cells for up to 83 passages. Four strains of SADS-CoV/GDWT-P7, -P18, -P48 and -P83 were isolated and characterized. Sequence alignments showed that these four novel strains exhibited 16 nucleotide mutations and resultant 10 amino acid substitutions in open reading frame 1a/1b, spike, NS3a, envelope, membrane and nucleocapsid proteins. Furthermore, a 58-bp deletion in NS7a/7b was found in P48 and P83 strains, which led to the loss of NS7b and 38 amino acid changes of NS7a. Pig infection studies showed that the P7 strain caused typical watery diarrhea, while the P83 strain induced none-to-mild, delayed and transient diarrhea. This is the first report on cell adaption of a virulent SADS-CoV strain, which gives information on the potential virulence determinants of SADS-CoV.

1. Introduction

Swine acute diarrhea syndrome coronavirus (SADS-CoV), also known as porcine enteric alphacoronavirus (PEAV) or swine enteric alphacoronavirus (SeACoV), is a newly emerging porcine coronavirus and is the etiological agent of swine acute diarrhea syndrome (SADS), which can cause severe and acute diarrhea and high mortalities among neonatal piglets in China (Gong et al., 2017; Pan et al., 2017; Zhou et al., 2018a). SADS-CoV is an enveloped, positive and single-stranded sense RNA virus that belongs to genus *Alphacoronavirus* in the family *Coronaviridae* of the order *Nidovirales* (Zhou et al., 2018a). The SADS-CoV genome is approximately 27 kb and contains nine open reading frame (ORFs) that are ORF1a, ORF1b, spike (S), envelope (E), membrane (M), nucleocapsid (N) and three accessory genes, NS3a, NS7a and NS7b (Zhou et al., 2018a; Wang et al., 2019).

In 2017, SADS-CoV infection broke out in Guangdong Province of China and resulted in the death of around 25, 000 piglets within a few months (Zhou et al., 2018a). At that time, some farms used the virus solution collected from intestines of infected piglets to feed pregnant sows orally, to a certain degree which prevented the spread of SADS-CoV. However, SADS-CoV re-emerged in Guangdong on February 2019 and led to the death of around 2000 piglets in one farm (Zhou et al., 2019a). So, there is an urgent need to isolate attenuated strains and develop vaccines to control SADS-CoV in pigs in China. Actually, the best way to prevent virus infection is vaccination of pregnant sows, which can induce lactogenic immunity, and their transmission to suckling piglets via colostrum and milk, are critical for early passive protection (Chattha et al., 2015). Like SADS-CoV, porcine epidemic diarrhea virus (PEDV) is also an enteric alphacoronavirus in pigs, but it can cause diarrhea to pigs of all ages and widespread in the world. To control PEDV, many live attenuated vaccines have been manufactured and licensed, for example, 83P-5 (Sato et al., 2011), attenuated CV77 (Sun et al., 2016), DR13 (Park et al., 2012), and SM98 (Kim et al., 2015). And more PEDV vaccine candidates including PEDVPT-P96 (Chang et al., 2017), PC22A-derived strains (Lin et al., 2017), PEDV YN-144 (Chen et al., 2015), Zhejinag08 (Li et al., 2017), iPEDVPT-P96 (Kao et al., 2018), and VSVMT-SΔ19 (Ke et al., 2019) also have been developed by serial cell passaging, cDNA clone construction or recombinant attenuated virus vector. As a newly discovered alphacoronavirus, recent studies regarding SADS-CoV have been mainly focused on molecular epidemiology, diagnosis, and experimental infection models (Fu et al., 2018; Zhoub et al. 2018, 2019; Xu et al., 2019), while

[*] Corresponding author.
[**] Corresponding author.
E-mail addresses: lantian2016@scau.edu.cn (T. Lan), majy2400@scau.edu.cn (J.Y. Ma).
[1] These authors contributed equally to this work.

https://doi.org/10.1016/j.virol.2019.09.009
Received 19 June 2019; Received in revised form 16 September 2019; Accepted 18 September 2019
Available online 21 September 2019
0042-6822/

information on SADS-CoV attenuation and vaccine development is yet to be obtained. The emergence and re-emergence of SADS-CoV have posted a great threat to the pig industry in China, which make it necessary to generate vaccines to prevent and control SASD-CoV infection.

In the present study, we reported the attenuation of a virulent strain SADS-CoV/CN/GDWT/2017 via serial propagation in Vero cells for up to 83 passages. The pathogenicity of SADS-CoV/GDWT-P7 and -P83 was evaluated in 6-day-old piglets and genetic variations related to attenuation were also identified by comparing full-genome sequences of SADS-CoV/GDWT-P7, -P18, -P48 and -P83. Our results indicated the virulent strain SADS-CoV/CN/GDWT/2017 was successfully attenuated and the SADS-CoV/GDWT-P83 strain could be further studied as attenuated vaccine candidate against SADS-CoV in China.

2. Materials and methods

2.1. Cells, animals and virus strain

African green monkey kidney cells (Vero cells) were kept in our laboratory and cultured in Dulbecco's modified Eagle's medium (DMEM, HyClone) supplemented with 10% fetal bovine serum (FBS, HyClone) at 37 °C within 5% CO_2 incubator. The SADS-CoV/CN/GDWT/2017 strain (GenBank accession number MG557844) was isolated from diarrhea samples of suckling piglets in a commercial pig farm in Guangdong Province in April 2017 (Zhou[a] et al., 2018) and was kept in our laboratory. 26 five-day-old healthy piglets that didn't suck colostrum after birth were purchased form a commercial farm in Guangdong with no history of SADS. All piglets were tested negative for SADS-CoV, PEDV, porcine deltacoronavirus (PDCoV), pseudorabies virus (PRV), rotavirus (RV) and transmissible gastroenteritis virus (TGEV) by virus-specific qPCRs on rectal swabs, and were detected antibody negative for porcine reproductive and respiratory syndrome virus (PRRSV) (Li et al., 2013; Mai et al., 2017; Wu et al., 2017; Zhou et al., 2019a,b).

2.2. Serial passage of the virus

Vero cells were cultured to 80%–90% confluence and washed three times with phosphate-buffered saline (PBS) (20% w/v). Then, cells were infected with the SADS-CoV/CN/GDWT/2017 strain and incubated with serum-free DMEM containing 10 μg/ml trypsin (Gibco). Infected cells were maintained at 37 °C with 5% CO_2 and monitored daily for cytopathic effects (CPE). When 90% of the cells showed CPE, cells were harvested, frozen and thawed three times, and centrifuged for 10 min at 8000 × *g*. The supernatant was collected and stored at −80 °C as the stock for the next passage. Using the same manner, 82 subsequent passages were conducted in Vero cells. Beginning at the 8th passage in cell culture, the virus was plaque purified every ten passages. The viral stocks every five or ten generations were titrated by performing a 10-fold serial dilution of supernatants in 96-well plates in triplicate per dilution, and the virus titration was determined by $TCID_{50}$ method (Reed and Muench, 1938).

2.3. Genome sequencing, alignment and phylogenetic analysis

The complete genomes of SADS-CoV isolates were amplified using previously reported primer pairs (Zhou et al., 2019a,b). PCR assays were performed with the following thermal profile: 95 °C for 3 min, 30 cycles of 95 °C for 30 s, 55 °C for 30 s, and 72 °C for 60 s, followed by a final 10 min extension at 72 °C. The products were purified following the manufacturer's instructions of Gel Band Purification Kit (Takara, China) and then cloned into the pMD19-T vector (Takara, China) and transformed E. coli DH5α competent cells. The positive clones were screened out and sent to Beijing Genomics Institute (Shenzhen, China) for further sequencing. The nucleotide sequences were assembled and aligned using the DNASTAR program (DNAStar V7.1, Madison, WI, USA). Phylogenetic trees were constructed using the neighbor-joining method in MEGA 7.0 software with bootstrap analysis of 1000 replicates. Percentages of replicate trees in which the associated taxa clustered are shown as nearby branches (Chenna et al., 2003; Tamura et al., 2004; Kumar et al., 2016).

2.4. Animal experiment design

26 piglets were randomly divided into three groups including two SADS-CoV- infected groups each containing nine piglets and one control group with eight piglets. After one day of acclimation, piglets in two inoculated groups were orally with 12 mL of $10^{6.3}$ $TCID_{50}$/mL of SADS-CoV/CN/WT/2017-P7 and -P83, respectively. Piglets in the control group were mock-inoculated in parallel with 12 mL of DMEM. Fecal consistency and body weight for each piglet were recorded or scored daily. Rectal swabs were also collected every day to detect viral shedding. When diarrhea was observed in infected groups, three piglets in each group were randomly selected to euthanized and necropsied to collect tissue samples for further analyses.

2.5. RNA extraction and qRT-PCR analysis

SADS-CoV RNA was extracted from fecal or tissue samples following the manufacturer's recommendations of AxyPrep™ Body Fluid Viral DNA/RNA Miniprep Kit (Axygen Scientific, Inc). Reverse transcription was carried out to synthetized cDNA according to the manufacturer's protocol of Prime ScriptTM RT Reagent Kit with gDNA Eraser (Takara, China). The TaqMan-based qRT-PCR assay established by our lab (Zhou et al., 2018b) was employed to amplify cDNA with specific primers (forward: 5' - CAGGTCTTGGTGTTCGCAATCG-3'; reverse: 5'- ACCGTG CTGAACGAGGTCACT-3'), and probe (5'-FAM- TCACAGTCTCGTTCTC GCAATCA-TAMRA-3') under the following protocol: 95 °C for 30 s for initial denaturation followed by 45 cycles of 95 °C for 5 s and 62 °C for 30 s. Ten-fold serial dilutions of the pMD19-T-SADS-CoV-N plasmid were used to generate a standard curve. The viral genomic copy numbers were calculated by comparing 1 μl of cDNA with a standard sample.

2.6. Histopathology and immunohistochemical staining

Tissue samples including duodenum, jejunum and ileum collected from the challenged and mock-infected piglets were fixed in 10% formalin for 24 h at room temperature, then dehydrated in graded ethanol, embedded in paraffin, and cut to 3 μm sections (Leica, Germany). The paraffin-embedded samples were deparaffinized in xylene, and washed in decreasing concentrations of ethanol. After that, the deparaffinized intestinal tissue sections were stained with hematoxylin and eosin (Sangon, China) for histopathology or subjected to immunohistochemistry assay using SADS-CoV-specific mouse antisera (1:400) and goat anti-mouse IgG (H + L)/HRP (1:50) through procedures described previously with some modifications (Zhou et al., 2018a).

3. Results

3.1. Biological and growth characteristics of the virus strain in serial of passages

During the serial propagation, viral titers of passage (P) 12, 23, 33, 38, 48, 53, 58, 63, 68, 73 and 83 were measured. The result showed that infectious titer of the passaged virus ranged from 10^4 to $10^{7.5}$ $TCID_{50}$/mL and rose sharply before P38, then slowed down and reached the highest titer at P83 (Fig. 1). As the same time, with the increase of the passage, CPE appeared more quickly. In P7-infected Vero cells, CPE appeared on 24 h post infection (hpi) including syncytial and vacuole formation, while over 90% of P83-infected cells died and floated at this

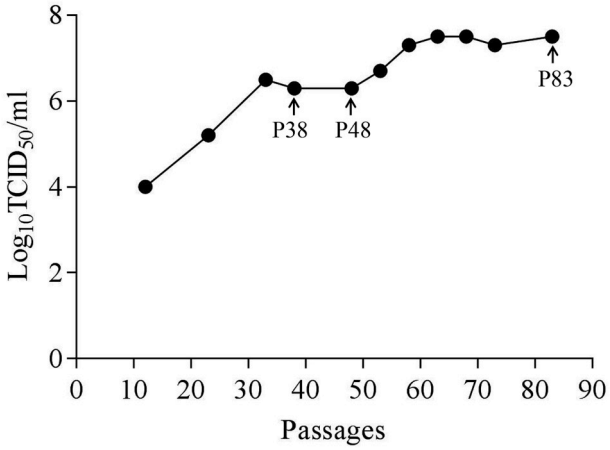

Fig. 1. Viral titers of SADS-CoV/CN/GDWT/2017 strain propagated in Vero cells after serial passage.

timepoint (Fig. 2). These results indicated an increasing adaptability for the virus in cell serial passage.

3.2. Sequence analysis

Four new complete genomes of SADS-CoV/GDWT-P7, -P18, -P48 and -P83 strains (accession number MK994934 to MK994937) were sequenced and available in GenBank. The length for the complete genomes of SADS-CoV/GDWT-P7 and -P18 stains was 27165 bp, and that of SADS-CoV/GDWT-P48 and -P83 was 27107 bp. Sequence alignments showed nucleotide identities between all available SADS-CoV genomes ranged from 99.3% to 100%. The four novel full-length sequences shared high nucleotide identities of 99.9%–100% with each other and 99.5%–100% with other reported complete genomes of SADS-CoV. Phylogenetic analyses based on complete genomes demonstrated that all SADS-CoV strains clustered together to form a well-defined group and separated from other alphacoronaviruses (Fig. 3).

After comparing full-length sequences of four new strains with that of SADS-CoV/CN/GDWT/2017, no insertion events were observed, but 16 nucleotide (nt) point mutations and the resultant 10 amino acid (aa) substitutions were found (Table 1). The ORF1a/1b had most mutations containing 9 nt and 5 aa changes, followed by S and N gene each harboring 2 nt and 1 aa changes. The E, M and NS3a had one aa substitution, respectively. Besides these mutations, a large deletion of 58 bp was found in SADS-CoV/GDWT-P48 and -P83. This 58 bp-deletion led to the loss of initial codons for both NS7a and NS7b and a reading frame shift for NS7a. As a result, the NS7b gene was lost in genomes of these two high-passage strains. For the Ns7a gene, the reading frame moved forward and caused an overlap of 107bp between the N and the NS7a. Finally, 20 additional aa were encoded and 18 aa substitutions were substituted in the initial part of NS7a (Fig. 4).

3.3. Pathogenicity difference between the low- and the high-passage strains

To explore whether these mutations and deletions of amino acids in high-passage strains can lead to virulence changes, SADS-CoV/GDWT-P7 (group A) and SADS-CoV/GDWT-P83 (group B) at same $TCID_{50}$ value were inoculated into six-day-old piglets. Clinical scoring of fecal consistency in challenged and control groups were shown in Table 2. At one day post-inoculation (DPI), all piglets (9/9) in the SADS-CoV/GDWT-P7-inoculated group presented with typical SADS-CoV-associated, loose-to-watery diarrhea. And the diarrhea peaked on 2–3 DPI (score ≥ 2), accompanying with watery feces ejecting from wet, red and swollen anus. Piglets were dispirited, not moving and even vomiting. The clinical signs lasted for six days. At 7 DPI, piglets began to recover and diarrhea disappeared. On the contrary, only two piglets (B3 and B6) in the SADS-CoV/GDWT-P83-inoculated group developed loose-to-semi-fluid diarrhea (score ≤ 2) on 5 DPI, and rapidly recovered on 7 DPI. The other piglets in this group showed no obvious clinical symptoms. In the mock-infected group, no clinical signs of diarrhea were observed.

The mean body weight in each group was investigated to assess clinical effects of diarrhea resulted by SADS-CoV/GDWT-P7 and -P83 infections in piglets. As shown in Fig. 5, piglets in the control group obviously weighed more than piglets in two challenged groups. Contrary to mock-infected piglets continuously gaining the body weight, piglets in SADS-CoV/GDWT-P7-infected group almost stopped growing on 1–2 DPI. After that the body weight began to slowly increase. For piglets inoculated by the SADS-CoV/GDWT-P83 strain, the body weight was basically same with that of the control group within three days after challenging, but nearly didn't alter in the following days, and on 5 DPI started to increase again.

The results of rectal swabs collected from SADS-CoV/GDWT-P7-inoculated group showed that SADS-CoV was detected positively from 2 to 7 DPI, which was approximately consistent with that of diarrheal clinical signs. Although the moderate diarrheal symptom of a piglet (A9) disappeared after 3 DPI, SADS-CoV was still detected positively from the rectal swab of this piglet until 7 DPI. In the SADS-CoV/GDWT-P83-inoculated group, rectal swabs from six piglets were detected positive for SADS-CoV, and the number was more than that of piglets with clinical signs of diarrhea. The piglet numbered B3 with the moderate diarrhea was detected positive for SADS-CoV from 2 to 5 DPI; it was the longest duration of viral shedding in this group. Three piglets including two euthanized were detected negative for SADS-CoV during the experiment. All piglets in the control group were also negative for SADS-CoV (Table 3).

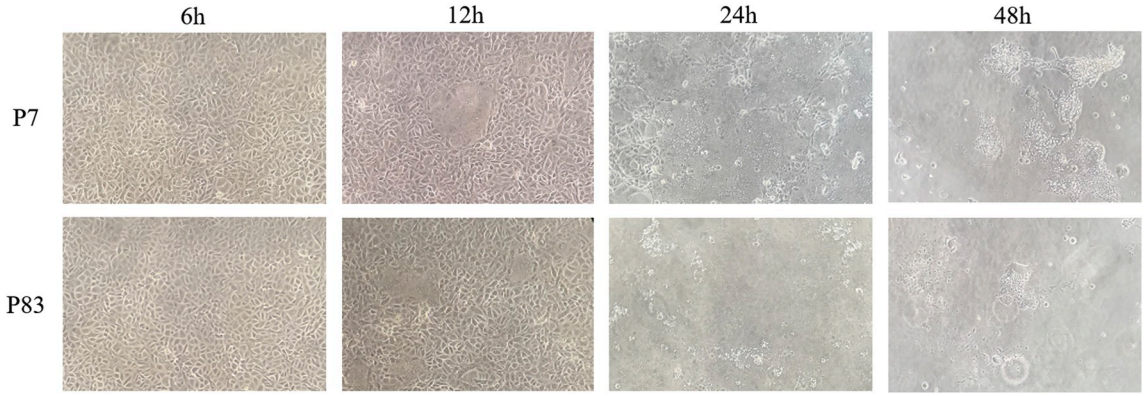

Fig. 2. Cytopathic effects (CPE) caused by SADS-CoV/CN/GDWT/2017-P7 or -P83 (100 ×). Vero cells were seeded into T-25 flasks and infected at a multiplicity of infection (MOI) of 0.01.

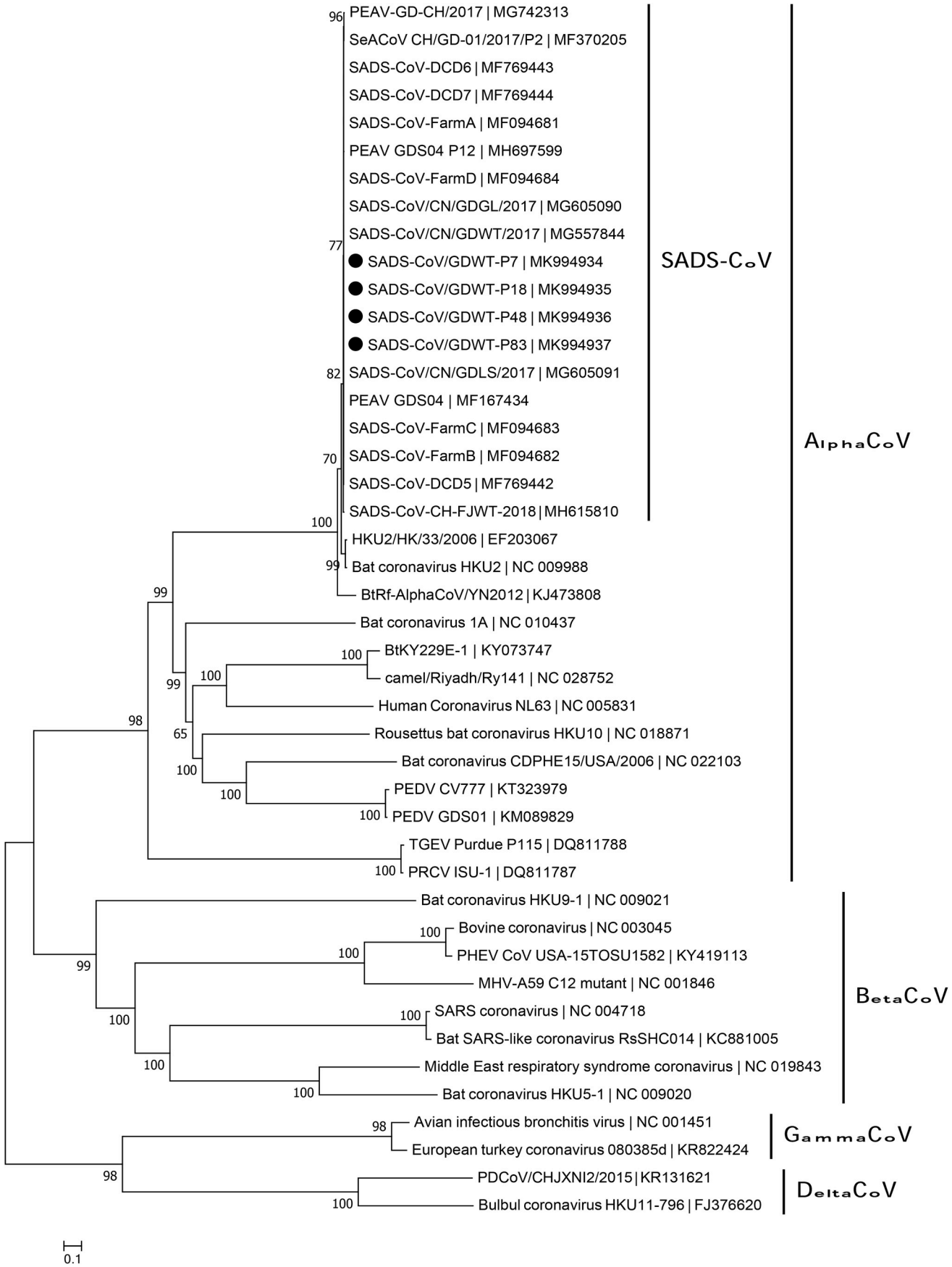

Fig. 3. Phylogenetic analysis of the complete genome of SADS-CoV and reference coronavirus species. The tree was constructed using MEGA 7.0 software with neighbor-joining methods and 1000 replicate sets on bootstrap analysis. Four new complete genomes sequences studied in this work were indicated with “black blots”.

Table 1
Changes in nucleotides and amino acids in SADS-CoV/GDWT-P7, -P18, -P48 and -P83 strains.

Gene		Nucleotide Change						Amino Acid Substitution
		Position	SASADS-CoV/CN/GDWT/2017	P7	P18	P48	P83	
OFR1a	NSP2	683	C	C	T	T	T	A17V
	NSP3	3838	G	G	G	T	T	A131S
	NSP3~NSP4	6230	T	T	T	C	C	L→S
	NSP4	7832	A	A	A	G	G	D47G
	NSP6	10242	C	C	C	T	T	–
	NSP6	10737	A	A	C	C	C	–
	NSP6	10831	G	G	G	A	A	V266I
	NSP9	11994	T	T	T	G	G	–
OFR1b	NSP10~NSP11	16763	C	C	C	T	T	–
S	S1	21166	T	T	T	T	C	–
	S2	22497	A	A	A	C	C	E671A
NS3a		23987	C	A	A	A	A	P37H
E		24678	G	G	G	T	T	R44 M
M		24832	C	C	T	T	T	L17F
N		26131	C	C	C	T	T	A217V
		26447	C	C	C	C	T	–

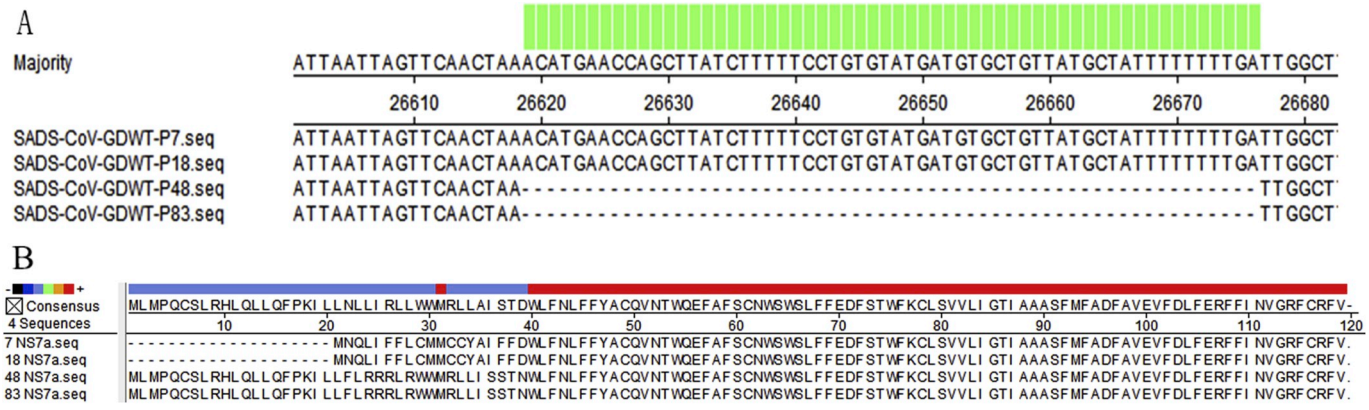

Fig. 4. Alignments of NS7a/7b genes of SADS-CoV/GDWT-P7, -P18, -P48 and -P83. A, the green solid boxes indicate the location of a 58 bp-deletion in P48 and P83 strains. B, the light blue regions indicate amino acid changes of NS7a proteins of P48 and P83 strains. (For interpretation of the references to colour in this figure legend, the reader is referred to the Web version of this article.)

Table 2
Clinical scoring of diarrhea. The scores were graded as follows: 0, normal; 1, loose diarrhea; 2, semi-fluid diarrhea; and 3, watery diarrhea. DPI, days post-inoculation.

DPI	SADS-CoV/GDWT-P7-inoculated group									SADS-CoV/GDWT-P83-inoculated group									Mock-infected gourp							
	A1	A2	A3	A4	A5	A6	A7	A8	A9	B1	B2	B3	B4	B5	B6	B7	B8	B9	C1	C2	C3	C4	C5	C6	C7	C8
0	0	0	0	0	0	0	0	0	0	0	0	0	0	0	0	0	0	0	0	0	0	0	0	0	0	0
1	3	3	1	3	3	2	1	2	1	0	0	0	0	0	0	0	0	0	0	0	0	0	0	0	0	0
2	3	3	2	3	3	3	2	3	2	0	0	0	0	0	0	0	0	0	0	0	0	0	0	0	0	0
3	3	3	3	3	3	1	2	3	1	0	0	0	0	0	0	0	0	0	0	0	0	0	0	0	0	0
4	3	/	2	2	/	0	1	/	0	/	0	0	0	/	0	/	0	0	0	/	0	0	/	0	0	/
5	2	/	1	1	/	0	0	/	0	/	0	2	0	/	1	/	0	0	0	/	0	0	/	0	0	/
6	1	/	0	0	/	0	0	/	0	/	0	1	0	/	0	/	0	0	0	/	0	0	/	0	0	/
7	0	/	0	0	/	0	0	/	0	/	0	0	0	/	0	/	0	0	0	/	0	0	/	0	0	/
8	0	/	0	0	/	0	0	/	0	/	0	0	0	/	0	/	0	0	0	/	0	0	/	0	0	/
9	0	/	0	0	/	0	0	/	0	/	0	0	0	/	0	/	0	0	0	/	0	0	/	0	0	/

/, A2, A5, A8, B1, B5, B7, C2, C5 and C8 were euthanized and necropsied for collecting tissue samples.

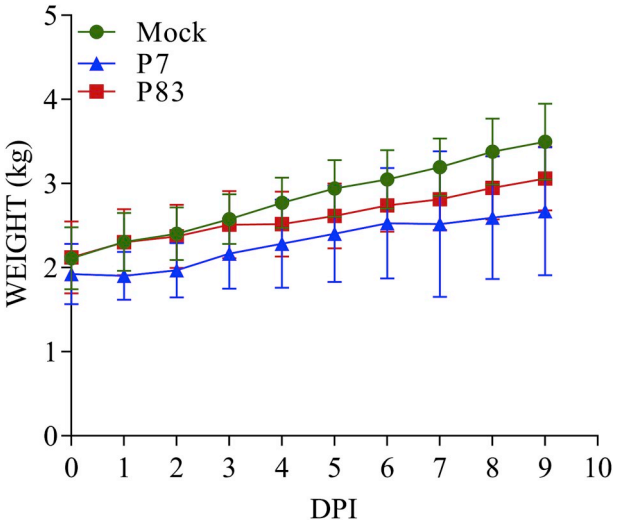

Fig. 5. Daily change in the body weight of 6-day-old piglets after SADS-CoV/GDWT-P7 or -P83 inoculation. The daily differences in mean body weight for each group were shown as mean ± standard error of the mean (SEM).

3.4. Tissue tropism

Twelve tissue samples including heart, liver, spleen, lung, kidney, tonsil, stomach, duodenum, jejunum, ileum, mesenteric lymph node and inguinal lymph node were collected to determine the different tissue tropism between the low- and high-passage. For the low-passage, P7 strain, viral RNA could be detected in samples of tonsils, stomach, duodenum, jejunum, ileum and mesenteric lymph nodes, among which the ileum had the highest viral load of 4.77log10 copies/μL. However, the viral RNA of the SADS-CoV/GDWT-P83, was only detected in ileum and mesenteric lymph nodes and with same viral copies of 1.67log10 copies/μL (Fig. 6).

3.5. Gross pathology, histopathology, and immunohistochemistry

The intestinal wall of small intestine of piglets inoculated by the SADS-CoV/GDWT-P7 strain became thinner, permeable, and the intestine was filled with a large number of yellow water feces. The digestive contents in the cecum and colon were also watery and without pigmentation. Mesenteric congestion was obvious and accompanied by individual bleeding points. While in SADS-CoV/GDWT-P83-inoculated piglets, thick intestinal wall, normal mesentery and pigmentation were observed, which was almost similar with those of mock-infected piglets (Fig. 7).

Histological changes associated with SADS-CoV infection were observed in the duodenum, jejunum and ileum samples collected from SADS-CoV/GDWT-P7-inoculated group. As shown in Fig. 8, SADS-CoV/GDWT-P7-infected piglets had clear histologic lesions with villus blunting and atrophying, nuclei dissolving and shedding, mucosal inflammatory cells increasing and sever adhesion between villi. While the normal villous epithelium was overserved in piglets in SADS-CoV/GDWT-P83-inoculated group and the mock-infected group. Consistent with the histological results, SADS-CoV antigen signals appeared brown and were detected in epithelial cells in the duodenum, jejunum and ileum of SADS-CoV/GDWT-P7-inoculated piglets. No SADS-CoV antigens were detected in samples of piglets inoculated with SADS-CoV/GDWT-P83 or mock-inoculated piglets (Fig. 9).

4. Discussion

As a newly emerging porcine enteric coronavirus, research on SADS-CoV attenuation has not been reported yet. Considering its high pathogenicity, there is an urgent need to isolate attenuated strains and develop efficient vaccines to control SADS-CoV. In the present study, for the first time we serially propagated the virulent strain SADS-CoV/CN/GDWT/2017 in Vero cells for up to 83 passages. Four novel strains SADS-CoV/GDWT-P7, -P18, -P48 and -P83 were successfully isolated and their genetic and pathogenic characteristics were ascertained. Compared to SADS-CoV/GDWT-P7-inoucalted piglets, SADS-CoV/GDWT-P83-inoculated piglets showed a mild and transient diarrhea with shorter viral shedding, weakened tissue tropism and undetected histopathological lesion, which provides evidence of viral attenuation and highlights SADS-CoV/GDWT-P83 strain as a potential, live-attenuated SADS-CoV vaccine candidate.

Entire genomes of these four isolated strains were sequenced to decode genetic changes that emerged during serial cell passage. By comparing with the sequence of SADS-CoV/CN/GDWT/2017, nucleotide mutations in ORF1a/b, N, S, E, M and NS3a were identified. Our result showed that half of the non-silent mutations (5/10) were located in the ORF1a gene, i.e. NSP2, NSP3, NSP4 and NSP6. It is well known that the NSPs of coronaviruses are associated with viral replications, many of which are considered to be interferon antagonists (Xing et al., 2013; Chang et al., 2017). Previous findings of PEDV attenuation also revealed relatively large nucleotide changes in ORF1a/1b (Chen et al., 2015; Lee et al., 2017), which suggests this may be a common feature for both SADS-CoV and PEDV. As a major surface protein, the coronavirus S protein possesses two subunits S1 and S2, which are responsible for cell receptor interaction and cell membrane fusion, respectively (Hulswit et al., 2016). In the present study, only one nucleotide mutation and resultant one amino acid substitution was found in the S2 region, and no insertion or deletion was observed in S gene, which were different with the discovery of PEDV. Some cell culture-attenuated PEDV strains, e.g., PEDV YN-144 (Chen et al., 2015), PEDVPT-P96 (Chang et al., 2017) and PC22A-derived strains (Lin et al., 2017), had many or most of amino acid changes in the region of S gene. Insertion mutations that resulted in four amino acid changes were found in the S1 region of cell culture-passaged PEDV CH/HNPJ/2016 strains (Liu et al., 2019). However, there was also no nucleotide change observed in S gene of attenuated PED-CUP-B2014 strain (Park et al., 2018). These results indicated multiple mutation patterns of virus attenuation during cell passaging. For SADS-CoV, more analyses are needed to explore potential molecular mechanisms of attenuation to provide valuable data for vaccine developments.

Besides structural and non-structural proteins, the genome of SADS-CoV also encodes three accessory genes, NS3a, NS7a and NS7b (Zhou et al., 2018a; Wang et al., 2019). NS3a locates between S and E protein, corresponding to ORF3 in PEDV genome or ORF3a/b in TGEV genome (Zuñiga et al., 2016; Wang et al., 2019). Many groups have demonstrated that cell-adapted PEDV or TGEV strains display either internal truncation or amino acid changes in the ORF3 gene, which suggests that ORF3 is of key importance for virus adaption and virulence attenuation (Zhang et al., 2007; Park et al., 2012; Jengarn et al., 2015; Wongthida et al., 2017). Similar to these findings, we observed the amino variation in the NS3a region of SADS-CoV/GDWT-P7 and other three new isolated strains, and we also noticed that the pathogenicity of P7-infected piglets was lower than that of the wild type SADS-COV strain. Although presenting typical SADS-CoV-associated diarrhea, P7-innoculated piglets survived and recovered in a week. The amino variation of NS3a in our assay seems to contribute to the virulence attenuation, which need further analysis to confirm the link between NS3a and attenuation of SADS-CoV.

During serial cell passage of the present study, the largest nucleotide changes, a 58 bp-deletion, occurred in NS7a and NS7b of SADS-CoV/GDWT-P48 and -P83 strains. This deletion led to the loss of NSA7b protein expression and the 38 amino acid-change of NS7a protein. Generally, the deletion of accessory genes could result in attenuated viruses, such as ORF7 deletion in TGEV (Ortego et al., 2003) and ORF7a/b deletion in feline infectious peritonitis virus (FIPV) (Haijema

Table 3
Viral shedding of experimental piglets after SADS-CoV inoculation analyzed by qPCR. +, positive; -, negative. CT value of 35 is considered as the threshold. DPI, days post-inoculation.

DPI	SADS-CoV/GDWT-P7-inoculated group									SADS-CoV/GDWT-P83-inocualted group		
	A1	A2	A3	A4	A5	A6	A7	A8	A9	B1	B2	B3
0	-/40.00	-/40.00	-/40.00	-/40.00	-/40.00	-/40.00	-/40.00	-/40.00	-/40.00	-/40.00	-/40.00	-/40.00
1	+/23.91	+/28.27	+/34.47	+/25.87	+/24.72	+/32.74	+/26.62	+/25.94	+/25.20	-/40.00	-/38.95	-/40.00
2	+/26.27	+/29.09	+/30.32	+/31.53	+/30.13	-/37.94	+/26.86	+/26.91	+/29.93	-/38.85	-/40.00	+/31.38
3	+/28.66	+/27.28	+/32.26	+/27.71	+/31.08	-/38.36	+/32.68	+/25.21	+/28.36	+/33.35	+/34.91	+/33.08
4	+/31.44	/	-/38.64	+/29.09	/	-/40.00	+/28.61	/	+/29.89	/	-/40.00	-/37.39
5	+/28.06	/	-/40.00	+/26.73	/	-/40.00	+/23.95	/	+/26.00	/	-/40.00	+/29.25
6	+/31.97	/	-/40.00	+/34.72	/	-/40.00	+/26.91	/	+/27.66	/	-/40.00	-/40.00
7	-/40.00	/	-/38.31	-/40.00	/	-/40.00	-/37.26	/	+/34.60	/	-/40.00	-/40.00
8	-/40.00	/	-/40.00	-/40.00	/	-/40.00	-/40.00	/	-/40.00	/	-/40.00	-/40.00
9	-/40.00	/	-/40.00	-/40.00	/	-/40.00	-/38.67	/	-/38.95	/	-/40.00	-/40.00

DPI	SADS-CoV/GDWT-P83-inocualted group						Mock-infected gourp						
	B4	B5	B6	B7	B8	B9	C1	C2	C3	C4	C5	C6	C7
0	-/40.00	-/40.00	-/40.00	-/40.00	-/40.00	-/40.00	-/40.00	-/40.00	-/40.00	-/40.00	-/40.00	-/40.00	-/40.00
1	-/40.00	-/39.01	-/40.00	-/40.00	-/40.00	-/40.00	-/40.00	-/40.00	-/39.94	-/40.00	-/40.00	-/40.00	-/40.00
2	-/40.00	-/40.00	-/40.00	-/38.36	-/40.00	-/40.00	-/40.00	-/40.00	-/38.52	-/40.00	-/40.00	-/40.00	-/40.00
3	-/40.00	-/40.00	-/40.00	-/40.00	-/38.18	-/36.63	-/40.00	-/40.00	-/40.00	-/40.00	-/40.00	-/40.00	-/40.00
4	+/34.01	/	+/34.13	/	-/38.49	+/34.39	-/40.00	/	-/37.78	-/40.00	/	-/40.00	-/40.00
5	-/40.00	/	-/38.34	/	-/40.00	-/40.00	-/40.00	/	-/40.00	-/38.07	/	-/40.00	-/40.00
6	+/33.48	/	-/40.00	/	-/37.39	-/38.42	-/40.00	/	-/38.54	-/38.39	/	-/38.29	-/40.00
7	-/40.00	/	-/40.00	/	-/38.39	-/40.00	-/40.00	/	-/40.00	-/40.00	/	-/40.00	-/37.95
8	-/40.00	/	-/40.00	/	-/40.00	-/40.00	-/40.00	/	-/40.00	-/40.00	/	-/38.01	-/40.00
9	-/40.00	/	-/40.00	/	-/40.00	-/40.00	-/40.00	/	-/40.00	-/40.00	/	-/40.00	-/40.00

/, A2, A5, A8, B1, B5, B7, C2, C5 and C8 were euthanized and necropsied for collecting tissue samples.

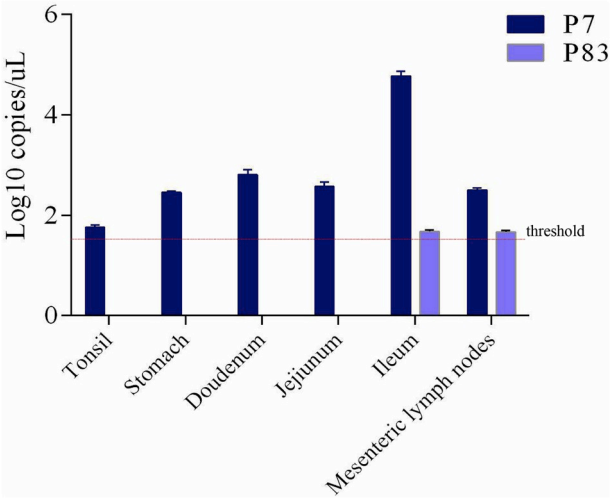

Fig. 6. Copy numbers of SADS-CoV genomes in different tissues of piglets infected by SADS-CoV/GDWT-P7 or -P83 strains at 4 DPI.

et al., 2004); but there was also a report that the virulence of ORF7-deleted TGEV was enhanced compared with that of parental viruses (Cruz et al., 2011). For SADS-CoV, as the total deletion of 7b protein and large substitutions of 7a protein appeared in the middle and late stage of cell passage, as well as the P83 strain presenting low virulence to piglets, we speculated that these changes in NS7a/7b may also contribute to the attenuation of SADS-CoV. In addition to virulence modulation, protein 7 also plays a role in interactions between virus infection and innate immunity. The absence of TGEV protein 7 increased expressions of IFN-β, IFN-stimulated genes and proinflammatory genes (Cruz et al., 2013). FIPV 7a protein acted as a type I IFN antagonist, when cooperating with ORF3-encoded proteins (Dedeurwaerder et al., 2014). Functions of protein 7 of SADS-CoV is necessary to study further to clarify its roles in cell adaption and virulence alteration. Collectively, our results showed that all nine ORFs of SADS-CoV exhibited nucleotide and amino acid changes during serial propagation, which indicates the attenuation of virus may be multifactorial. These variations mentioned above along the genome may constitute a combination to have an impact on cell adaptation and virulence attenuation of SADS-CoV, or it is possible that some individual mutations may have key determinants, all of which need more investigations by the reverse genetic method.

5. Conclusions

In summary, SADS-CoV/CN/GDWT/2017 was successfully attenuated through serial passaging in Vero cells as evidenced by enhanced virus titers in cells and reduced pathogenesis in neonatal piglets. Genetic investigations revealed that 10 non-silent mutations in ORF1a/1b, S, E, NS3a, M and N, and a 58-bp deletion in NS7a/7b contributed to cell adaption and virulence attenuation. To our knowledge, this is the first report to serial passage culture and attenuation investigation of a virulent SADS-CoV strain. The results of this study are important for mapping the virulence determinants of SADS-CoV and for the development of effective vaccines against SADS in China.

Declarations

Ethics approval and consent to participate

This study was carried out in accordance with the recommendations of National Standards for Laboratory Animals of the People's Republic of China (GB149258-2010). The protocol was approved by Animal Research Committees of South China Agricultural University. Pigs used for this study were handled in accordance with good animal practices required by the Animal Ethics Procedures and Guidelines of the People's Republic of China.

Availability of data and material

The data and material used and analyzed during the current study are available from the corresponding author on reasonable request. The serum and tissue samples used in the study were kept in the Poultry Laboratory of the College of Animal Science, South China Agricultural University.

Conflicts of interest

The authors report no conflicts of interest. The authors themselves are responsible for the content and writing of the paper.

Fundings

This work was supported by the Science and Technology Program of Guangzhou City of China (No. 201904010433), the Research and Extension of Major Animal Epidemic Prevention and Control Technologies in the Strategic Project of Rural Revitalization of Guangdong Agricultural Department of China (Building Modern Agricultural System) (2018–2020), and China Scholarship Council.

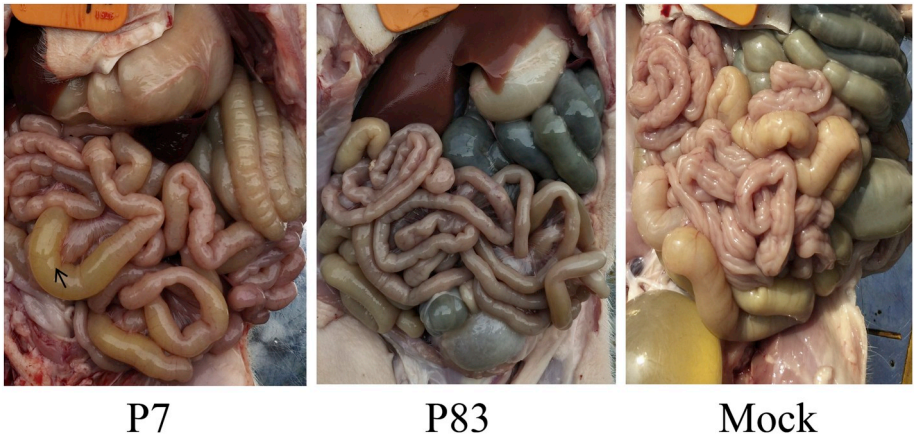

Fig. 7. Intestinal dissection of experimental piglets infected by SADS-CoV/GDWT-P7 or -P83 strains at 4 DPI. Thin-walled intestinal tract of containing yellow water feces was indicated by the arrow. (For interpretation of the references to colour in this figure legend, the reader is referred to the Web version of this article.)

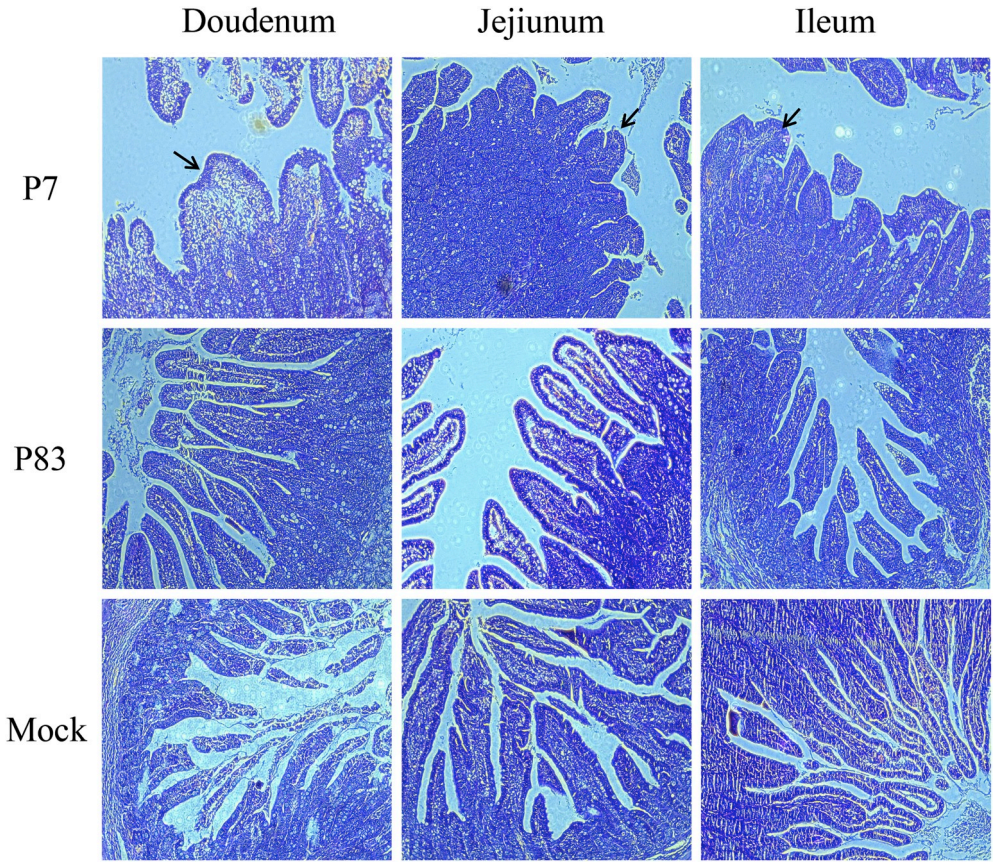

Fig. 8. H&E-stained intestinal tissue section of experimental piglets infected by SADS-CoV/GDWT-P7 or -P83 strains at 4 DPI. Blunt intestinal villus was indicated by arrows.

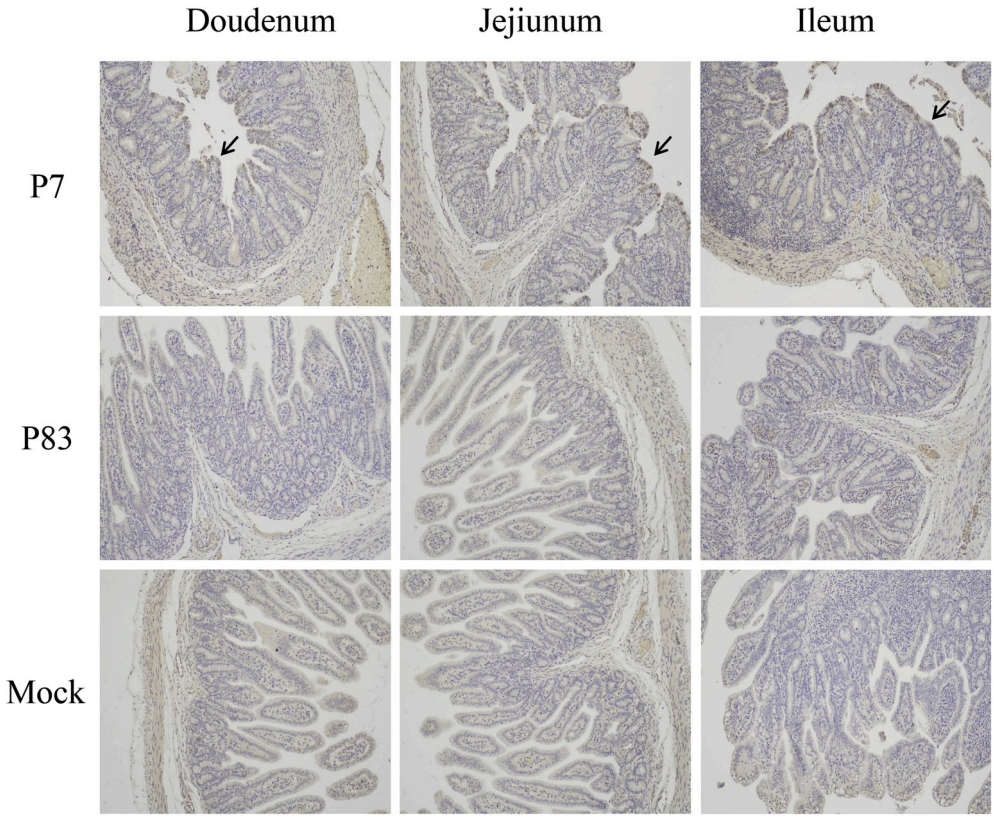

Fig. 9. Immunohistochemistry (IHC) of the small intestines of piglets inoculated with SADS-CoV/GDWT-P7 or -P83 strains at 4 DPI. Arrows indicate the antigen signals of SADS-CoV.

Authors' contributions

Conceptualization, JYM and TL; Data curation, YS, JC, YL, XLY and ZHZ; Methodology, JC, YL, ZXW, LLH and YRT; Formal analysis, YS, JC, YL and XLY; Funding acquisition, JYM; Investigation, JC, YL, ZXW, LLH and YRT; Project administration, JYM and TL; Resources, JYM and TL; Supervision, JYM and YS; Validation, QNL, LZ, and RTW; Visualization, JC and XLY; Writing – original draft, YS; Writing-review & editing, YS and JYM. All authors read and approved the final manuscript.

References

Chattha, K.S., Roth, J.A., Saif, L.J., 2015. Strategies for design and application of enteric vral vaccines. Annu. Rev. Anim. Biosci. 3, 6.1–6.21.

Chang, Y.C., Kao, C.F., Chang, C.Y., Jeng, C.R., Tsai, P.S., Pang, V.F., et al., 2017. Evaluation and comparison of the pathogenicity and host immune responses induced by a G2b Taiwan porcine epidemic diarrhea virus (strain Pintung 52) and its highly cell-culture passaged strain in conventional 5-week-old pigs. Viruses 9, 121. https://doi:10.3390/v9050121.

Chen, F., Zhu, Y., Wu, M., Ku, X., Ye, S., Li, Z., Guo, X., 2015. Comparative genomic analysis of classical and variant virulent parental/attenuated strains of porcine epidemic diarrhea virus. Viruses 7, 5525–5538.

Chenna, R., Sugawara, H., Koike, T., Lopez, R., Gibson, T.J., Higgins, D.G., Thompson, J.D., 2003. Multiple sequence alignment with the Clustal series of programs. Nucleic Acids Res. 31, 3497–3500.

Cruz, J.L.G., Sola, I., Becares, M., Alberca, B., Plana, J., Enjuanes, L., Zuñiga, S., 2011. Coronavirus gene 7 counteracts host defenses and modulates virus virulence. PLoS Pathog. 7 (6), e1002090.

Cruz, J.L.G., Becares, M., Sola, I., Oliveros, J.C., Enjuanes, L., Zúñigaa, S., 2013. Alphacoronavirus protein 7 modulates host innate immune response. J. Virol. 87, 9754–9767.

Dedeurwaerder, A., Olyslaegers, D.A.J., Desmarets, L.M.B., Roukaerts, I.D.M., Theuns, S., Nauwynck, H.J., 2014. ORF7-encoded accessory protein 7a of feline infectious peritonitis virus as a counteragent against IFN-a-induced antiviral response. J. Gen. Virol. 95, 393–402.

Fu, X., Fang, B., Liu, Y., Cai, M., Jun, J., Ma, J., et al., 2018. Newly emerged porcine enteric alphacoronavirus in southern China: identification, origin and evolutionary history analysis. Infect. Genet. Evol. 62, 179–187.

Gong, L., Li, J., Zhou, Q., Xu, Z., Chen, L., Zhang, Y., et al., 2017. A new bat-HKU2–like coronavirus in swine, China, 2017. Emerg. Infect. Dis. 23, 1607–1609.

Haijema, B.J., Volders, H., Rottier, P.J., 2004. Live, attenuated coronavirus vaccines through the directed deletion of group-specific genes provide protection against feline infectious peritonitis. J. Virol. 78, 3863–3870.

Hulswit, R.J.G., de Haan, C.A.M., Bosch, B.J., 2016. Coronavirus spike protein and tropism changes. Adv. Virus Res. 96, 29–57.

Jengarn, J., Wongthida, P., Wanasen, N., Frantz, P.N., Wanitchang, A., Jongkaewwattana, A., 2015. Genetic manipulation of porcine epidemic diarrhoea virus recovered from a full-length infectious cDNA clone. J. Gen. Virol. 96, 2206–2218.

Kao, C.F., Chiou, H.Y., Chang, Y.C., Hsueh, C.S., Jeng, C.R., Tsai, P.S., et al., 2018. The characterization of immunoprotection induced by a cDNA clone derived from the attenuated Taiwan porcine epidemic diarrhea virus Pintung 52 Strain. Viruses 10, 543. https://doi:10.3390/v10100543.

Ke, Y., Yu, D., Zhang, F., Gao, J., Wang, X., Fang, X., Wang, H., 2019. Recombinant vesicular stomatitis virus expressing the spike protein of genotype 2b porcine epidemic diarrhea virus: a platform for vaccine development against emerging epidemic isolates. Virology 533, 77–85.

Kim, S.H., Lee, J.M., Jung, J., Kim, I.J., Hyun, B.H., Kim, H.I., et al., 2015. Genetic characterization of porcine epidemic diarrhea virus in Korea from 1998 to 2013. Arch. Virol. 160, 1055–1064.

Kumar, S., Stecher, G., Tamura, K., 2016. MEGA7: molecular Evolutionary Genetics analysis version 7.0 for bigger datasets. Mol. Biol. Evol. 33 (7), 1870–1874.

Lee, S., Son, K.Y., Noh, Y.H., Lee, S.C., Choi, H.W., Yoon, I.J., Lee, C., 2017. Genetic characteristics, pathogenicity, and immunogenicity associated with cell adaptation of a virulent genotype 2b porcine epidemic diarrhea virus. Vet. Microbiol. 207, 248–258.

Li, Z., Chen, F., Yuan, Y., Zeng, X., Wei, Z., Zhu, L., et al., 2013. Sequence and phylogenetic analysis of nucleocapsid genes of porcine epidemic diarrhea virus (PEDV) strains in China. Arch. Virol. 158, 1267–1273.

Li, Y., Wang, G., Wang, J., Man, K., Yang, Q., 2017. Cell attenuated porcine epidemic diarrhea virus strain Zhejiang08 provides effective immune protection attributed to dendritic cell stimulation. Vaccine 35 (50), 7033–7041.

Lin, C.M., Hou, Y., Marthaler, D.G., Gao, X., Liu, X., Zheng, L., et al., 2017. Attenuation of an original US porcine epidemic diarrhea virus strain PC22A via serial cell culture passage. Vet. Microbiol. 201, 62–71.

Liu, X., Zhang, Q., Zhang, L., Zhou, P., Yang, J., Fang, Y., et al., 2019. A newly isolated Chinese virulent genotype GIIb porcine epidemic diarrhea virus strain: biological characteristics, pathogenicity and immune protective effects as an inactivated vaccine candidate. Virus Res. 259, 18–27.

Mai, K., Feng, J., Chen, G., Li, D., Zhou, L., Bai, Y., et al., 2017. The detection and phylogenetic analysis of porcine deltacoronavirus from Guangdong Province in Southern China. Transboundary Emerg. Dis. 65 (1), 166–173.

Ortego, J., Sola, I., Almazan, F., Ceriani, J.E., Riquelme, C., Balasch, M., et al., 2003. Transmissible gastroenteritis coronavirus gene 7 is not essential but influences in vivo virus replication and virulence. Virology 308, 13–22.

Pan, Y., Tian, X., Qin, P., Wang, B., Zhao, P., Yang, Y., et al., 2017. Discovery of a novel swine enteric alphacoronavirus (SeACoV) in southern China. Vet. Microbiol. 211, 15–21.

Park, S.J., Kim, H.K., Song, D.S., An, D.J., Park, B.K., 2012. Complete genome sequences of a Korean virulent porcine epidemic diarrhea virus and its attenuated counterpart. J. Virol. 86 (10), 5964.

Park, J.E., Kang, K.J., Ryu, J.H., Park, J.Y., ang, H., Sung, J.J., et al., 2018. Porcine epidemic diarrhea vaccine evaluation using a newly isolated strain from Korea. Vet. Microbiol. 221, 19–26.

Reed, L.J., Muench, H., 1938. A simple method of estimating fifty per cent endpoints. Am. J. Epidemiol. 27, 493–497.

Sato, T., Takeyama, N., Katsumata, A., Tuchiya, K., Kodama, T., Kusanagi, K., 2011. Mutations in the spike gene of porcine epidemic diarrhea virus associated with growth adaptation in vitro and attenuation of virulence in vivo. Virus Genes 43, 72–78.

Sun, D., Wang, X., Wei, S., Chen, J., Feng, L., 2016. Epidemiology and vaccine of porcine epidemic diarrhea virus in China: a mini-review. J. Vet. Med. Sci. 78, 355–363.

Tamura, K., Nei, M., Kumar, S., 2004. Prospects for inferring very large phylogenies by using the neighbor-joining method. Proc. Natl. Acad. Sci. 101, 11030–11035.

Wang, Q., Vlasova, A.N., Kenney, S.P., Saif, L.J., 2019. Emerging and re-emerging coronaviruses in pigs. Curr. Opin. Virol. 34, 39–49.

Wongthida, P., Liwnaree, B., Wanasen, N., Narkpuk, J., Jongkaewwattana1, A., 2017. The role of ORF3 accessory protein in replication of cell-adapted porcine epidemic diarrhea virus (PEDV). Achieve Virol. 162, 2553–2563.

Wu, Q., Zhao, X., Bai, Y., Sun, B., Xie, Q., Ma, J., 2017. The first identification and complete genome of Senecavirus A affecting pig with idiopathic vesicular disease in China. Transboundary Emerg. Dis. 64, 1633–1640.

Xing, Y., Chen, J., Tu, J., Zhang, B., Chen, X., Shi, H., et al., 2013. The papain-like protease of porcine epidemic diarrhea virus negatively regulates type I interferon pathway by acting as a viral deubiquitinase. J. Gen. Virol. 94, 1554–1567.

Xu, Z., Zhang, Y., Gong, L., Huang, L., Lin, Y., Qin, J., et al., 2019. Isolation and characterization of a highly pathogenic strain of Porcine enteric alphacoronavirus causing watery diarrhoea and high mortality in newborn piglets. Transboundary Emerg. Dis. 66, 119–130.

Zhang, X., Hasoksuz, M., Spiro, D., Halpin, R., Wang, S., Stollar, S., et al., 2007. Complete genomic sequences, a key residue in the spike protein and deletions in nonstructural protein 3b of US strains of the virulent and attenuated coronaviruses, transmissible gastroenteritis virus and porcine respiratory coronavirus. Virology 358, 424–435.

Zhou, P., Fan, H., Lan, T., Yang, X., Zhang, W., Zhu, Y., et al., 2018a. Fatal swine acute diarrhea syndrome caused by an HKU2-related coronavirus of bat origin. Nature 556, 255–258.

Zhou, L., Sun, Y., Wu, J., Mai, K., Chen, G., Wu, Z., et al., 2018b. Development of a TaqMan-based real-time RT-PCR assay for the detection of SADS-CoV associated with severe diarrhea disease in pigs. J. Virol Methods 255, 66–70.

Zhou, L., Li, Q.N., Su, J.N., Chen, G.H., Wu, Z.X., Luo, Y., et al., 2019a. The Re-emerging of SADS-CoV Infection in Pig Herds in Southern China. *Transboundary And Emerging Diseases*. accepted.

Zhou, L., Sun, Y., Lan, T., Wu, R., Chen, J., Wu, Z., et al., 2019b. Retrospective detection and phylogenetic analysis of swine acute diarrhoea syndrome coronavirus in pigs in southern China. Transboundary Emerg. Dis. 66 (2), 687–695.

Zuñiga, S., Pascual-Iglesias, A., Sanchez, C.M., Sola, I., Enjuanes, L., 2016. Virulence factors in porcine coronaviruses and vaccine design. Virus Res. 226, 142–151.

Abbreviations

SADS-CoV: swine acute diarrhea syndrome coronavirus
SADS: swine acute diarrhea syndrome
PEAV: porcine enteric alphacoronavirus
SeACoV: swine enteric alphacoronavirus
ORF: open reading frame
S: spike
E: envelope
M: membrane
N: nucleocapsid
PEDV: porcine epidemic diarrhea virus
PDCoV: porcine deltacoronavirus
PRRSV: porcine reproductive and respiratory syndrome virus
PRV: porcine pseudorabies virus
RV: rotavirus
TGEV: transmissible gastroenteritis virus
PBS: phosphate-buffered saline;
CPE: cytopathic effects
hpi: h post infection
DPI: day post-inoculation